



Silicon nanocluster sensitization of erbium ions under low-energy optical excitation

Nikola Prtljaga, Daniel Navarro-Urrios, Alessandro Pitanti, Federico Ferrarese-Lupi, Blas Garrido et al.

Citation: *J. Appl. Phys.* **111**, 094314 (2012); doi: 10.1063/1.4712626

View online: <http://dx.doi.org/10.1063/1.4712626>

View Table of Contents: <http://jap.aip.org/resource/1/JAPIAU/v111/i9>

Published by the [American Institute of Physics](#).

Related Articles

Dopant effects on the photoluminescence of interstitial-related centers in ion implanted silicon
J. Appl. Phys. **111**, 094910 (2012)

Above-room-temperature photoluminescence from a strain-compensated Ge/Si_{0.15}Ge_{0.85} multiple-quantum-well structure
Appl. Phys. Lett. **100**, 141905 (2012)

Capability of photoluminescence for characterization of multi-crystalline silicon
J. Appl. Phys. **111**, 073504 (2012)

Investigation of defect states in heavily dislocated thin silicon films
J. Appl. Phys. **111**, 053706 (2012)

Temperature dependence of the indirect bandgap in ultrathin strained silicon on insulator layer
Appl. Phys. Lett. **100**, 102107 (2012)

Additional information on J. Appl. Phys.

Journal Homepage: <http://jap.aip.org/>

Journal Information: http://jap.aip.org/about/about_the_journal

Top downloads: http://jap.aip.org/features/most_downloaded

Information for Authors: <http://jap.aip.org/authors>

ADVERTISEMENT

AIP Advances

Special Topic Section:
PHYSICS OF CANCER

Why cancer? Why physics?

[View Articles Now](#)

Silicon nanocluster sensitization of erbium ions under low-energy optical excitation

Nikola Prtljaga,^{1,a)} Daniel Navarro-Urrios,^{2,b)} Alessandro Pitanti,³ Federico Ferrarese-Lupi,⁴ Blas Garrido,⁴ and Lorenzo Pavesi¹

¹*NanoScience Lab, Department of Physics, University of Trento, Via Sommarive 14, 38123 Povo, Trento, Italy*

²*Phononic and Photonic Nanostructure Group, CIN2-CSIC, Campus Bellaterra – Edifici CM3, 08193 Bellaterra, Barcelona, Spain*

³*NEST, Scuola Normale Superiore, Istituto di Nanoscience – CNR, Piazza di San Silvestro 12, 56 127 Pisa, Italy*

⁴*MIND-IN2UB, Departament D’Electrònica, Universitat de Barcelona, Carrer Martí i Franqués, 08 028 Barcelona, Spain*

(Received 8 January 2012; accepted 5 April 2012; published online 10 May 2012)

The sensitizing action of amorphous silicon nanoclusters on erbium ions in thin silica films has been studied under low-energy (long wavelength) optical excitation. Profound differences in fast visible and infrared emission dynamics have been found with respect to the high-energy (short wavelength) case. These findings point out to a strong dependence of the energy transfer process on the optical excitation energy. Total inhibition of energy transfer to erbium states higher than the first excited state ($^4I_{13/2}$) has been demonstrated for excitation energy below 1.82 eV (excitation wavelength longer than 680 nm). Direct excitation of erbium ions to the first excited state ($^4I_{13/2}$) has been confirmed to be the dominant energy transfer mechanism over the whole spectral range of optical excitation used (540 nm–680 nm). © 2012 American Institute of Physics.

[<http://dx.doi.org/10.1063/1.4712626>]

I. INTRODUCTION

The discovery of the sensitizing action of silicon nanocluster (Si-nc) on erbium ions (Er^{3+}) offered a new material platform where silicon based optical amplifiers and laser sources could be developed.¹ Complementary metal oxide semiconductor (CMOS) process compatibility combined with convenient light emission in the third telecom window ($1.5 \mu m$) has been considered as a particular advantage of this material.² In spite of promising initial reports of optical gain³ and efficient electrical excitation,⁴ the demonstration of a laser action seems still to be quite challenging. While a number of limiting factors to stimulated emission have been identified,^{5–8} the estimates of their impact on laser action are still imprecise, partially owing to difficulties encountered when modeling the energy transfer mechanism.^{9–11} Although, the transfer mechanism between Si-nc and Er^{3+} has been thoroughly studied,^{7,11,12} there is no clear consensus in literature on the more appropriate model to describe this interaction. Most of the studies have been performed with optical excitation in the high energy spectral region (blue, UV) where the absorption cross section of Si-nc is dominating that of the Er^{3+} ions.^{13,14} Excitation at longer wavelengths (lower energies), where the absorption cross section of these two materials becomes comparable, may provide a valuable insight in the energy transfer mechanism.^{11,15–18}

^{a)}nikolap@science.unitn.it.

^{b)}Present address: Catalan Institute of Nanotechnology (CIN2-CSIC), Campus UAB, Edifici CM3, 08193 Bellaterra, Spain.

II. EXPERIMENTAL DETAILS

We report on a photoluminescence (PL) study of silicon rich oxide thin films co-doped with Er^{3+} ions (SRO: Er^{3+}), under low-energy optical excitation. The general features of the PL dynamics are studied by time resolved photoluminescence (TR PL) measurements, performed both in the visible and in the infrared.

Samples are produced by reactive magnetron co-sputtering. Detailed description of fabrication details can be found in Ref. 19. The sample details are summarized in Table I. Photoluminescence measurements were done using, as an excitation source, the optical pulses (6 ns pulse length, 10 Hz repetition rate) of an optical parametric oscillator (OPO) pumped with the third harmonic of a Nd:YAG laser. The excitation photon flux ($10^{24} \text{ ph cm}^{-2} \text{ s}^{-1}$) was maintained constant over the whole used spectral range. Continuous wave (CW) PL measurements were performed using the 476 nm line of an Argon laser ($3 \times 10^{20} \text{ ph cm}^{-2} \text{ s}^{-1}$). Detection consisted of a spectrograph (Chromex) coupled to a streak camera (Hamamatsu, visible) or of a monochromator (Chromex) coupled to an InGaAs photomultiplier (Hamamatsu, infrared) with overall time resolution of 2 ns (visible) and 40 ns (infrared), respectively. All measurements were performed at room temperature. All spectra were corrected for the spectral response of the instruments.

These samples have been previously systematically characterized under a short wavelength excitations (355 nm, 476 nm), pulsed and continuous.⁷ Based on these results, a model describing the energy interaction between Si-nc and Er^{3+} in this (high energy) regime was proposed.¹⁰

TABLE I. Sample specifications.

Deposition method		RF reactive magnetron sputtering	
Sample name	Si excess (%)	Er ³⁺ ($\times 10^{20} \text{ cm}^{-3}$)	Annealing temperature (°C)
A	5 ± 2	3.4 ± 0.2	900
B	6 ± 2	...	900

III. RESULTS AND DISCUSSION

When optically exciting this material (with energy not matching any of the possible internal transitions of Er³⁺ ions, see Fig. 1), the pump photons are absorbed by the silicon nanoclusters and the energy is subsequently transferred to the Er³⁺ ions. Recently, it has been demonstrated that this energy transfer occurs on a very short temporal scale.^{6,10,12} As a consequence of the energy transfer, the exciton population in Si-nc is decreased, leading to a quenching of the visible PL (originating from Si-nc) in the Er³⁺ doped sample.¹⁰

In our samples, we monitor the visible PL dynamic (at 750 nm) in the first 400 ns after the laser pulse arrival, by using a 50 ns time gate (Fig. 2) in order to filter out any initial fast contribution that might not be due to radiative inter-band exciton recombination in Si-nc. We observe that although there is a clear difference in the emission dynamic for the two samples (A and B, see Table I) with a “blue” pump (470 nm), the dynamics becomes equal moving towards the “red” (640 nm) (Fig. 2).

It is important to underline that the difference in the emission dynamic of the two samples under “blue” pump condition does not necessarily imply that the energy transfer from Si-nc to Er³⁺ is still occurring on the timescale of observation (≈ 100 ns). In fact, it was demonstrated recently that the energy transfer could be a very fast process,^{6,10,12} taking place typically on the timescale shorter than 100 ns (Ref. 6) (<36 ns in our samples).¹⁰ On the other hand, the exciton recombination dynamics in Si-nc depends heavily on the exciton population itself, due to effects such as Auger

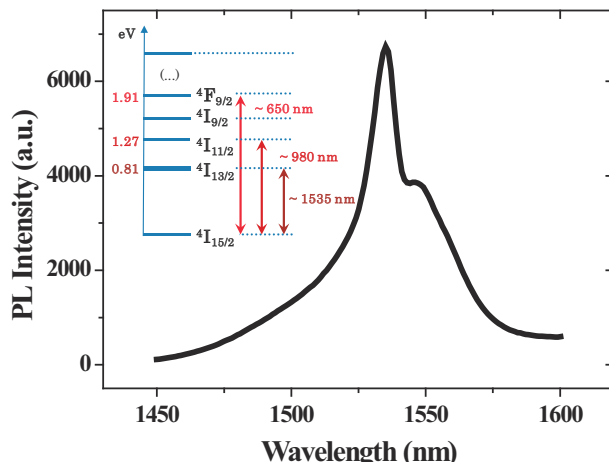


FIG. 1. Spectrum of the $^4I_{13/2} - ^4I_{15/2}$ transition of Er³⁺ ions (transition from the first excited state to the ground state) under non-resonant (476 nm) continuous optical excitation. Inset: Er³⁺ energy states scheme with Russell-Saunders notation and characteristic radiative transitions.

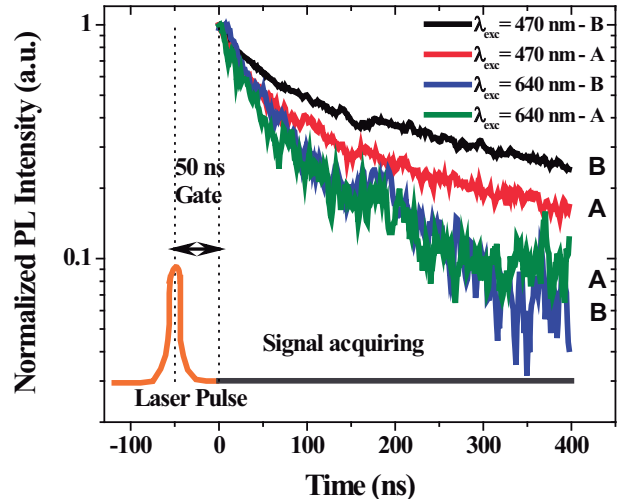


FIG. 2. Fast decay dynamics of the visible PL of samples A (red and green line) and B (black and blue line) under 470 nm excitation (upper two lines) and 640 nm (lower two lines). The time decay traces were recorded at 750 nm using a 90 nm wide spectral window. 50 ns time gate (inset) was used in order to filter out the initial fast contribution.

recombination²⁰ and inter-nanocluster transport.^{21,22} This is well illustrated in the Fig. 2 if we consider the emission dynamic of the *same* sample under two *different* excitation conditions (“blue” and “red”). Although, approximately, the same excitation photon fluxes were used (see Experimental Details), the wavelength dependence of the absorption cross-section¹³ of the Si-nc leads to different exciton populations and different fast ($<\mu\text{s}$) emission dynamics.

The difference in emission dynamics we observe between *different* samples (A and B) under the *same* (“blue”) pump condition is an indicator of a different exciton population in the two samples. This difference is not related to a change in the absorption cross-section (as we are using the same pump conditions), but to the Er³⁺ ions presence.^{13,14} As already mentioned previously, Er³⁺ ions are introduced in our samples during the deposition phase,¹⁹ minimizing, therefore, the occurrence of erbium related defect states.²³ Hence, we associate the difference in emission dynamics (exciton population) with the energy transfer mechanism present in erbium co-doped sample.²⁴

However, if we consider the *different* samples (A and B) under the *same* “red” pump condition (Fig. 2) the emission dynamics (exciton populations) we observe are practically the same. As it is rather unlikely that non-radiative recombination due to Er³⁺ related defect states show such a strong dependence on excitation wavelength in this range of energies,^{23,25} we attribute this distinct behavior to a *change* in the energy transfer process.

In order to investigate further this phenomenon, we monitor the initial PL dynamics of the $^4I_{13/2} - ^4I_{15/2}$ transition of Er³⁺ ions (at 1535 nm, transition from the first excited to fundamental state, see Fig. 1) while changing the excitation wavelength in the spectral range (540 nm–680 nm) around the value of the “red” pump previously used (640 nm).²⁶

In the literature, the dynamics of the $^4I_{13/2} - ^4I_{15/2}$ transition is frequently described by an initial microseconds PL rise followed by a very slow PL decay (on millisecond time

scale, 5.5 ms in our sample) (see Fig. 3).^{6,7} The latter is due to the radiative $^4I_{13/2} - ^4I_{15/2}$ transition and, in the absence of detrimental effects such as cooperative up-conversion, it is independent on the excitation photon flux.²⁷ On the other hand, the initial microseconds rise dynamic is considered to be due to the internal relaxation from high energy states of Er³⁺ to the $^4I_{13/2}$ state.^{7,11,28} The higher energy states of Er³⁺ are indirectly populated by the energy transfer process. Although the first tens of ns are hidden by a very fast PL decay contribution (Fig. 3, inset), it is evident that the μ s PL rise does not start from a zero level. This implies that a fraction of the Er³⁺ ions have been excited through the energy transfer process directly to the first excited state.^{7,11,28}

The very fast PL decay contribution (Fig. 3, inset), in our samples, has been experimentally related to the presence of the silicon nanoclusters (silicon excess) in the silicon dioxide matrix^{7,10,29} in accordance with what reported in Ref. 30. However, based on similar experimental findings, an alternative interpretation involving Er³⁺ $^4I_{13/2} - ^4I_{15/2}$ radiative transition and Er³⁺ related traps has been proposed.^{6,23} Considering that the contribution of this component to the total PL is practically negligible and that the elucidation of its exact origin falls out of the scope of this work, it will not be investigated further.

In order to quantify the relative contributions of the direct and higher state energy transfer contributions to the total PL, we fit the experimental data with the equation (see Appendix for more details)

$$I_{PL}(t) = I_{Background} + A_{All} \exp[-(t - t_0)/t_2] - A_{Slow} \exp[-(t - t_0)/t_1], \quad (1)$$

where $I_{Background}$ (background level) and t_0 (laser pulse arrival time) are fit parameters, $t_1 = 4.2 \mu\text{s}$ and $t_2 = 5.5 \text{ ms}$ have been independently measured.¹⁰ The other fit parameters are A_{Slow} and A_{All} (A_{Fast} being $A_{All} - A_{Slow}$). Their graphical

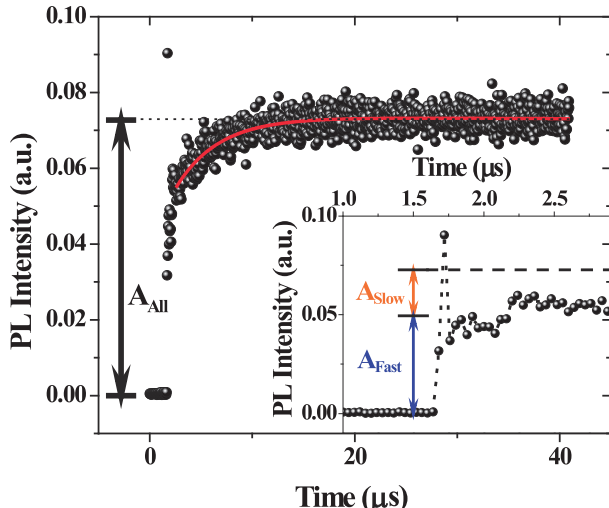


FIG. 3. Initial PL dynamics of the $^4I_{13/2} - ^4I_{15/2}$ transition of Er³⁺ ions under 560 nm pulsed excitation (black spheres). The best fit by Eq. (1) (red line) of the experimental data is also shown. The meaning of the fit parameter A_{All} is illustrated as well. Inset: Zoom on the first μ s of the initial PL dynamics. Graphical interpretation of the fit parameters A_{Slow} and A_{Fast} is shown.

interpretation is presented in Fig. 3. A_{Slow} weights the electronic contribution to the first excited state coming from the internal relaxation from higher energy states while A_{Fast} represents the direct contribution to the first excited state. A_{All} is simply the sum of the two, or in other words, the total contribution to the first excited state.

More insight on the underlying physics could be gained by the plot of the ratio A_{Fast}/A_{All} (see Fig. 4 and inset of Fig. 4), which yields an estimate of the “fast” direct contribution (given by A_{Fast}) to the total excited Er³⁺ population, as a function of the excitation wavelength.³¹

We observe a non-monotonic dependence of the A_{Fast}/A_{All} ratio upon excitation wavelength (see Fig. 4). For excitation wavelength shorter than 600 nm, a saturation region where the ratio is almost independent of the excitation photon wavelength is found. On the contrary, for longer excitation wavelengths, the ratio is increasing, and reaches a value of one for 680 nm excitation independently of the photon flux (within the limits imposed by our experimental setup). The antiresonant feature at 650 nm is related with the direct resonant excitation of Er³⁺ ions to $^4F_{9/2}$ energy state (see Fig. 1). Indeed, in this case we observe an increase of the “slow” contribution (given by A_{Slow}), leading to a decrease of the ratio A_{Fast}/A_{All} . Note that resonant features at shorter wavelengths are not observed, since the energy transfer to high Er³⁺ states becomes more efficient than the direct excitation.

A ratio of one corresponds to a complete absence of the contribution from higher lying states to the Er³⁺ $^4I_{13/2}$ state. In other words, energy transfer from Si-nc to higher excited states of Er³⁺ is not allowed any more at the excitation

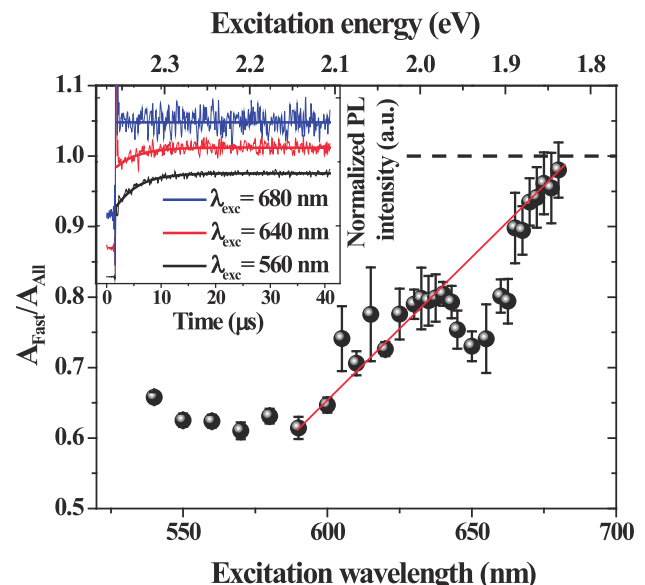


FIG. 4. Variation of the A_{Fast}/A_{All} ratio (black spheres) with the excitation wavelength. The black dashed line represents the value at which no contribution from higher excited state of Er³⁺ ions is present. The red solid line is only a guideline for the eyes. Inset: Initial PL dynamics of the $^4I_{13/2} - ^4I_{15/2}$ transition of Er³⁺ ions under 560 nm (thin black bottom curve), 640 nm (thin red middle curve), and 680 nm (thin blue upper curve) pulsed excitation. The best fits by Eq. (1) (thick lines of corresponding color) of the experimental data are also shown. The data and fit curves have been normalized and offset by 0.2 for clarity.

energy of 1.82 eV, where the excess energy with respect to the second excited state of Er^{3+} is approximately 0.55 eV. It is worth noticing that transition to this state is rather smooth, taking place for the excitation energies in the range between 2.1 and 1.8 eV (see Fig. 4). Moreover, a part from the change in its initial dynamics (Fig. 2), visible PL coming from the Si-nc is still observable.

These observations could be associated with the intraband model for the energy transfer.^{10,11} In this model, intraband electronic transitions are responsible for the energy transfer to Er^{3+} and, in particular, they require a minimum excess energy corresponding to a bandgap value of silicon nanoclusters.^{10,11} However, it comes as a surprise the relatively small amount of the measured excess energy values needed for the transfer to occur towards the $^4I_{11/2}$ state (0.8–0.55 eV). These values are lower than the expected bandgap energy of silicon nanoclusters in our samples (≈ 1.6 eV)³² and even lower than the bulk crystalline silicon bandgap (≈ 1.1 eV), indicating a participation of a sub-bandgap state in the energy transfer process.¹⁰

Sub-bandgap states have been theoretically predicted in amorphous Si-nc with low hydrogen content.³³ In addition, a modest spread in energy has been suggested to occur for weakly localized states due to limited effects of quantum confinement.³³

It should be mentioned, that recently, it has been postulated, as well, the possible existence of deep trap states related with presence of Er^{3+} ions in the bulk silicon.²⁵

An alternative explanation to our experimental observations would be that we have two different types of sensitizers present in our samples. As the absorption cross-section of the silicon nanoclusters is decreasing with wavelength, the effective cross-section of Er^{3+} ions sensitization through the Si-nc may reach a lower value, where the contribution from another sensitizer type could become significant.

The influence of Er related matrix defects on Er^{3+} photoluminescence has been demonstrated recently, but in very different energy range.²³ On the other hand, the silicon excess related “luminescence center” erbium sensitization has been well established in a wide range of excitation energies.^{15,29} However, an even distribution in the energy of these defect states is expected,^{15,28,29} with wavelength dependence of effective cross-section for erbium sensitization mirroring one of the silicon nanoclusters.¹⁵ Moreover, the energy transfer to higher energy states of Er^{3+} ions would be still possible for this sensitizing mechanism at the excitation energies we use,^{12,28–30} in contrast to what we observe.

To address this issue, we report in Fig. 5 A_{Fast} (direct contribution to the first excited state) as a function of the excitation energy (wavelength). A continuous monotonic decrease can be observed across the whole excitation range suggesting the existence of only one erbium sensitizer which we relate to Si-nc.¹³

The presence of a saturation region below 600 nm (see Fig. 4) with a value of $A_{\text{Fast}}/A_{\text{All}}$ ratio equal to 0.6 implies that direct energy transfer to the first excited state remains to be a dominant excitation mechanism even under short wavelength excitation.

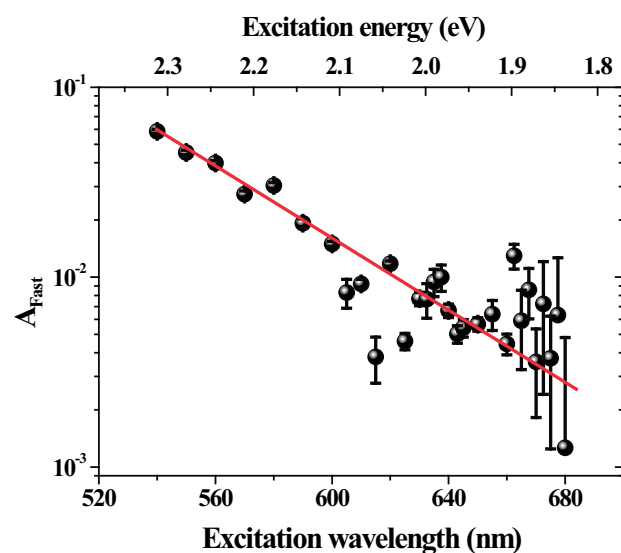


FIG. 5. A_{Fast} (direct contribution to the first excited state of Er^{3+} ions) dependence on the excitation wavelength (black spheres). The red solid line is only a guideline for the eyes.

IV. CONCLUSIONS

In conclusion, we reported a systematic study of the energy transfer process in silicon nanoclusters and Er^{3+} co-doped thin films under low energy optical excitation. The study presented here complements a recent work focused on PL quantum yield of SRO:Er³⁺ material under similar excitation conditions.¹⁸ We find profound differences in the fast dynamic of the visible PL with respect to the high energy optical excitation regime which we attribute to a decrease of the energy transfer efficiency and/or decrease of excitation to higher (than first) excited states of Er^{3+} . We demonstrate that the energy transfer to a higher energy state of Er^{3+} ions ceases to be effective for photon energies between 2.1 and 1.8 eV (0.7–0.55 eV of pump excess energy with respect to the energy of $^4I_{11/2}$ state). We explain this behavior in the framework of the intraband model in terms of sub-bandgap states participation in the energy transfer. Although we do not provide the definitive proof of their physical nature, we correlate them with the presence of Si-nc. We confirm that the energy transfer to the first excited state of Er^{3+} remains to be a dominant excitation mechanism in the range of considered excitation energies, implying that even with the opening of the new excitation channels, through the higher Er^{3+} excited states, only modest improvements in the efficiency of the Er^{3+} ions excitation should be expected.

ACKNOWLEDGMENTS

The authors would like to thank R. Rizk and F. Gourbillau for the sample growth and Nicola Daldosso for the participation in early stages of this work. Authors acknowledge the financial support of the HELIOS Project (FP7 224312). D.N.U. acknowledges the financial support of AGAUR through the Beatriu de Pinós program.

APPENDIX: EQUATION 1 DERIVATION

The PL dynamics of the $^4I_{13/2} - ^4I_{15/2}$ transition of Er^{3+} ions (at 1535 nm, transition from the first excited to

fundamental state, see Fig. 1, main text) is characterized by two contributions (see Fig. 2, main text): a very fast direct one (on \approx ns timescale) and a slow (on $\approx\mu$ s timescale) process caused by the internal relaxation from higher excited states of Er^{3+} ions. The very fast decaying initial PL contribution is not considered since regardless of its origin, its contribution to the total PL intensity is insignificant. Therefore, the time evolution of the PL signal can be described by the following equation:

$$\begin{aligned} I_{PL}(t) = & I_{Background} + A_{Fast} \exp[-(t - t_0)/t_2] \\ & + A_{Slow} \{1 - \exp[-(t - t_0)/t_1]\} \exp(-[t - t_0]/t_2). \end{aligned} \quad (\text{A1})$$

$I_{Background}$ (background level) and t_0 (laser pulse arrival time) are fit parameters, $t_1 = 4.2 \mu\text{s}$ and $t_2 = 5.5 \text{ ms}$ are fixed quantities and have been independently measured.¹⁰ t_2 is the decay constant of the first excited state while t_1 is the measure of the internal relaxation time. The other fit parameters are A_{Slow} and A_{Fast} . A_{Fast} is the direct contribution to the total PL while A_{Slow} gives the contribution by the internal relaxation from higher energy states.

The first exponential term describes the PL signal evolution coming from the fraction of the Er^{3+} ions population that has been directly excited to the first excited state while the second term gives the PL signal of the Er^{3+} ions that has been excited to higher states. In this last case, PL follows an internal relaxation from the higher states to the first excited state. On the timescale of the observation, the amplitude of the later one is a function of time as the internal relaxation continues (Eq. (A1)) causing the complex exponential dependence of the PL signal in time.

We assumed that the direct excitation to the first (and higher) excited states is instantaneous (faster than the time resolution of our detection system \approx 40 ns) and that the relaxation from the higher excited states to the $^4I_{13/2}$ state can be well described by a decaying single exponential function with a characteristic time $t_1 = 4.2 \mu\text{s}$. Note that Eq. (A1) and parameter physical interpretation are different respect to what can be found in similar works.^{17,34}

By introducing the parameter A_{All} , which is the sum of the previous two contributions, or in other words, the total contribution to the first excited state

$$A_{All} = A_{Fast} + A_{Slow}. \quad (\text{A2})$$

Eq. (A1) could be rewritten as:

$$\begin{aligned} I_{PL}(t) = & I_{Background} + A_{Fast} \exp[-(t - t_0)/t_2] \\ & + A_{Slow} \exp[-(t - t_0)/t_2] \\ & - A_{Slow} \exp[-(t - t_0)/t_1] \exp[-(t - t_0)/t_2] \\ = & I_{Background} + A_{All} \exp[-(t - t_0)/t_2] \\ & - A_{Slow} \exp\{[t_2(t - t_0) + t_1(t - t_0)]/[t_1 t_2]\}. \end{aligned} \quad (\text{A3})$$

Knowing that t_1 is more than three orders of magnitude smaller than t_2 , Eq. (A3) can be simplified to

$$\begin{aligned} I_{PL}(t) = & I_{Background} + A_{All} \exp[-(t - t_0)/t_2] \\ & - A_{Slow} \exp[-(t - t_0)/t_1]. \end{aligned} \quad (\text{A4})$$

This form is the one used for the fitting procedure.

- ¹M. Fujii, M. Yoshida, Y. Kanzawa, S. Hayashi, and K. Yamamoto, *Appl. Phys. Lett.* **71**, 1198 (1997).
- ²D. Liang and J. E. Bowers, *Nat. Photonics* **4**, 511 (2010).
- ³H. S. Han, S. Y. Seo, and J. H. Shin, *Appl. Phys. Lett.* **79**, 4568 (2001).
- ⁴O. Jambois, F. Gourbilleau, A. J. Kenyon, J. Montserrat, R. Rizk, and B. Garrido, *Opt. Express* **18**, 2230 (2010).
- ⁵B. Garrido, C. García, S. Y. Seo, P. Pellegrino, D. Navarro-Urrios, N. Daldozzo, L. Pavese, F. Gourbilleau, and R. Rizk, *Phys. Rev. B* **76**, 245308 (2007).
- ⁶I. Izeddin, A. Moskalenko, I. Yassievich, M. Fujii, and T. Gregorkiewicz, *Phys. Rev. Lett.* **97**, 207401 (2006).
- ⁷D. Navarro-Urrios, A. Pitanti, N. Daldozzo, F. Gourbilleau, R. Rizk, B. Garrido, and L. Pavese, *Phys. Rev. B* **79**, 193312 (2009).
- ⁸C. J. Oton, W. H. Loh, and A. J. Kenyon, *Appl. Phys. Lett.* **89**, 031116 (2006).
- ⁹A. Kenyon, M. Wojdak, I. Ahmad, W. Loh, and C. Oton, *Phys. Rev. B* **77**, 035318 (2008).
- ¹⁰A. Pitanti, D. Navarro-Urrios, N. Prtljaga, N. Daldozzo, F. Gourbilleau, R. Rizk, B. Garrido, and L. Pavese, *J. Appl. Phys.* **108**, 053518 (2010).
- ¹¹I. Izeddin, D. Timmerman, T. Gregorkiewicz, A. Moskalenko, A. Prokofiev, I. Yassievich, and M. Fujii, *Phys. Rev. B* **78**, 035327 (2008).
- ¹²O. Savchyn, F. Ruhge, P. Kik, R. Todi, K. Coffey, H. Nukala, and H. Heinrich, *Phys. Rev. B* **76**, 195419 (2007).
- ¹³D. Kovalev, J. Diener, H. Heckler, G. Polisski, N. Künzner, and F. Koch, *Phys. Rev. B* **61**, 4485 (2000).
- ¹⁴F. Priolo, G. Franzò, D. Pacifici, V. Vinciguerra, F. Iacona, and A. Irrera, *J. Appl. Phys.* **89**, 264 (2001).
- ¹⁵O. Savchyn, R. M. Todi, K. R. Coffey, L. K. Ono, B. R. Cuenya, and P. G. Kik, *Appl. Phys. Lett.* **95**, 231109 (2009).
- ¹⁶D. Timmerman, I. Izeddin, P. Stallinga, I. N. Yassievich, and T. Gregorkiewicz, *Nat. Photonics* **2**, 105 (2008).
- ¹⁷M. Falconieri, E. Borsella, F. Enrichi, G. Franzò, F. Priolo, F. Iacona, F. Gourbilleau, and R. Rizk, *Opt. Mater.* **27**, 884 (2005).
- ¹⁸N. N. Ha, S. Cueff, K. Dohnalová, M. T. Trinh, C. Labbé, R. Rizk, I. N. Yassievich, and T. Gregorkiewicz, *Phys. Rev. B* **84**, 241308(R) (2011).
- ¹⁹L. Khomenkova, F. Gourbilleau, J. Cardin, and R. Rizk, *Physica E* **41**, 1048 (2009).
- ²⁰H. M'ghaieth, H. Maaref, I. Mihalcescu, and J. C. Vial, *Phys. Rev. B* **60**, 4450 (1999).
- ²¹L. Pavese and M. Ceschini, *Phys. Rev. B* **48**, 17625 (1993).
- ²²R. Lockwood, A. Hryciw, and A. Meldrum, *Appl. Phys. Lett.* **89**, 263112 (2006).
- ²³S. Saed, D. Timmerman, and T. Gregorkiewicz, *Phys. Rev. B* **83**, 155323 (2011).
- ²⁴S. Yerci, R. Li, S. O. Kucheyev, T. Van Buuren, S. N. Basu, and L. Dal Negro, *IEEE J. Sel. Top. Quantum Electron.* **16**(1), 114 (2010).
- ²⁵I. Izeddin, M. Klik, N. Vinh, M. Bresler, and T. Gregorkiewicz, *Phys. Rev. Lett.* **99**, 077401 (2007).
- ²⁶We measured as well the dynamics of the $^4I_{11/2} - ^4I_{15/2}$ transition of the Er^{3+} ions (at 980 nm, transition from the second excited to ground state, see Fig. 1). However, the analysis of this last is complicated by the weak signal under "red" excitation and by the high background noise due to residual Si-nc emission. Thus, these measurements are inconclusive and, as such, discarded from further consideration.
- ²⁷D. Navarro-Urrios, A. Pitanti, N. Daldozzo, F. Gourbilleau, L. Khomenkova, R. Rizk, and L. Pavese, *Physica E* **41**, 1029 (2009).
- ²⁸O. Savchyn, R. M. Todi, K. R. Coffey, and P. G. Kik, *Appl. Phys. Lett.* **94**, 241115 (2009).
- ²⁹S. Cueff, C. Labbé, B. Dierre, F. Fabri, T. Sekiguchi, X. Portier, and R. Rizk, *J. Appl. Phys.* **108**, 113504 (2010).
- ³⁰A. Al Choueiry, A. M. Jurdy, B. Jacquier, F. Gourbilleau, and R. Rizk, *J. Appl. Phys.* **106**, 053107 (2009).
- ³¹The same dependence is found even when t_1 is assumed to be a fit parameter. In this case, values of t_1 of the order of few μs are found as well.
- ³²Estimated from the peak of visible photoluminescence.
- ³³G. Allan, C. Delerue, and M. Lannoo, *Phys. Rev. Lett.* **78**, 3161 (1997).
- ³⁴M. Fujii, *J. Appl. Phys.* **95**, 272 (2004).